Bennert Machenhauer

Part 1: SLIDE 1-28 Diagnosis of Systematic Initial Tendency Errors using slow normal mode assimilation. Bennert Machenhauer and Ingo Kirchner

DIAGNOSIS OF SYSTEMATIC INITIAL TENDENCY ERRORS IN THE ECHAM4 AND ECHAM4.5 AGCMS USING SLOW NORMAL MODE ASSIMILATION OF ECMWF REANALYSIS (REA-15) DATA

Part 1 presented at the

Modes Workshop NCAR 25-28 Aug. 2015

by

Bennert Machenhauer and Ingo Kirchner

Work carried out at Max-Planck Institute for Meteorology, Hamburg

SINCE KLINKER AND SARDESHMUKH (1992) PUBLISHED THEIR METHOD TO DETERMINE SYSTEMATIC INITIAL TENDENCY ERRORS AND NEW IMPROVED REANALYSIS BECAME AVAILABLE IN THE FORM OF THE NEW REA-15 AND LATER THE PLANS FOR REA-40 WE HAVE BEEN INTERESTED IN TRYING TO USE IT TO IDENTIFY MODEL ERRORS IN OUR CLIMATE MODELS. THE GLOBAL (ECHAM) AND IF POSSIBLE ALSO OUR REGIONAL (HIRLAM) CLIMATE MODEL.

PURPOSE OF PART 1:

To prepare for the assimilation of REA-40 (T106,L60) into the ECHAM 5 (T42, L19)

(Neither the REA-40 nor the ECHAM5 were available when this Part 1 were carried out)

We had previously tried to use Klinker and Sadeshmukh's method to determine SITEs by assimilating the relatively high resolution reanalysis data ERA-15 (T106, L31), given 4 times a day, into the low resolution climate model ECHAM4/4.5, (T42, L19). We had realized the problems:

- **The necessary truncation from T106 to T42 and the vertical interpolation from 31 levels to 19 levels creates small scale noise in the data**

- **As the data were given only 4 times a day the daily solar cycle could not be resolved adequate at all places.**

Therefore two versions of a new "continuous" assimilation technique:

The "Slow Normal Mode Insertion (SNMI)" technique

were developed, tested and compared with a traditional nudging technique (DMI nudging), as described in the following Part 1.

Systematic Initial Tendency Errors (SITEs) determined by full insertion of all variables at four synoptic times (00,06,12,18 UTC)

(Klinker and Sardeshmukh, 1992, Eliasen and Machenhauer, 1969)

$$\left(\frac{\partial X_i}{\partial t}\right)^n = F_i^n\left(X_1^n, X_2^n, \ldots, X_M^n\right) \qquad (1)$$

$$Insert \quad X_i^n = X_{OBS,i}^n \text{ in } F_i^n$$

The Systematic Initial Tendency Error (SITE) is *then* defined :

$$SITE = \frac{1}{N}\sum_{n=1}^{N}\left[F_i^n\left(X_1^n, X_2^n, \ldots, X_M^n\right) - \frac{X_{OBS,i}^{n+1} - X_{OBS,i}^{n-1}}{2\Delta t}\right]$$

$$= \frac{1}{N}\sum_{n=1}^{N}\left[F_i^n\left(X_1^n, X_2^n, \ldots, X_M^n\right)\right] - \frac{X_{OBS,i}^{N+1} - X_{OBS,i}^{1}}{2N\Delta t}$$

SLIDE 2

i = index number of a certain prognostic variable

M = total number of prognostic variables

n = index number of a synoptic time

N = total number of synoptic time steps in a month (or a longer time period)

The traditional *NODGING* technique (Jeuken et al., 1996) is defined as follows:

$$\frac{\partial X_i}{\partial t} = F_i(X_1, X_2, \ldots, X_N) + G_i \times (X_{OBS,i} - X_i)$$

In a three level scheme :

$$X_i^{n+1} = X_i^{n-1} + 2\Delta t\, F_i^n(X_1^n, X_2^n, \ldots, X_M^n) + 2\Delta t\, G_i \times (X_{OBS,i}^{n+1} - X_i^{n+1})$$

or

$$X_i^{n+1} = \mu_i \times X_{OBS,i}^{n+1} + (1-\mu_i) \times X_{m,i}^{n+1} \quad (1)$$

where $\mu_i = \dfrac{2\Delta t\, G_i}{1 + 2\Delta t\, G_i}$ and

$$X_{m,i}^{n+1} = X_i^{n-1} + 2\Delta t\, F_i^n(X_1^n, X_2^n, \ldots, X_M^n)$$

The initial tendency error (ITE^n) is defined :

$$ITE^n = F_i^n(X_1^n, X_2^n, \ldots, X_M^n) - \frac{X_{OBS,i}^{n+1} - X_{OBS,i}^{n-1}}{2\Delta t}$$

and the SITE is again the $= \dfrac{1}{N}\sum_{n=1}^{N} ITE^n$

The SNMI scheme is a NODGING scheme. So, we shall at first introduce that scheme. In the NODGING scheme a nudging term, with a nudging coefficient G_i is added to the prognostic equation. In a three level scheme the equation may be written as shown in (1) where μ_i is a nudging weight for the variable X_i and $X_{OBS,i}^{n+1}$ is the cubic spline interpolated observed value at time (n+1) x Δ t. It is Interpolated between two synoptic times. $X_{m,i}^{n+1}$ is the freely forecasted value at time (n+1)xΔt. The SITE is then obtained by averaging over a month and subtracting the observed change divided by the time averaged over. (See last equation in SLIDE 2).

SNMI = SLOW NORMAL MODE INSERTION

Any model state X(t) can be split into two parts:
the SLOW NORMAL MODE PART: $[X(t)]_{slow}$ *(all modes with periods larger than 24 hours)*
and
the FAST NORMAL MODE PART: $([X(t)]_{fast})$ *(all modes with periods smaller thjan 24 hours)*
Thus we may write

$$X(t)=[X(t)]_{slow}+[X(t)]_{fast}$$

We wont to assimilate only the slow normal mode part of the ERA data so we insert

$$X_{OBS}^{n+1}=(X_{ERA}^{n+1})_{slow}+(X_m^{n+1})_{fast} \text{ and } X_m^{n+1}=(X_m^{n+1})_{slow}+(X_m^{n+1})_{fast}$$

Into (1) and get

$$X^{n+1}=[\mu(t) \times (X_{ERA}^{n+1})_{slow}+(1-\mu(t)) \times (X_m^{n+1})_{slow}]+[(X_m^{n+1})_{fast}] \qquad (2)$$

THUS, WE ARE NUDGING THE SLOW MODES TOWARDS THE ERA, WHEREAS THE FAST MODES ARE COMPLETELY FREE. I. E. THEY ARE FORECASTED BY THE MODEL WITHOUT ANY NODING TOWARD THE ERA. IF μ = 1 THE QUPIC SPLINE INTERPOLATED SLOW NORMAL MODES ARE INSERTED EVERY TIMESTEP.

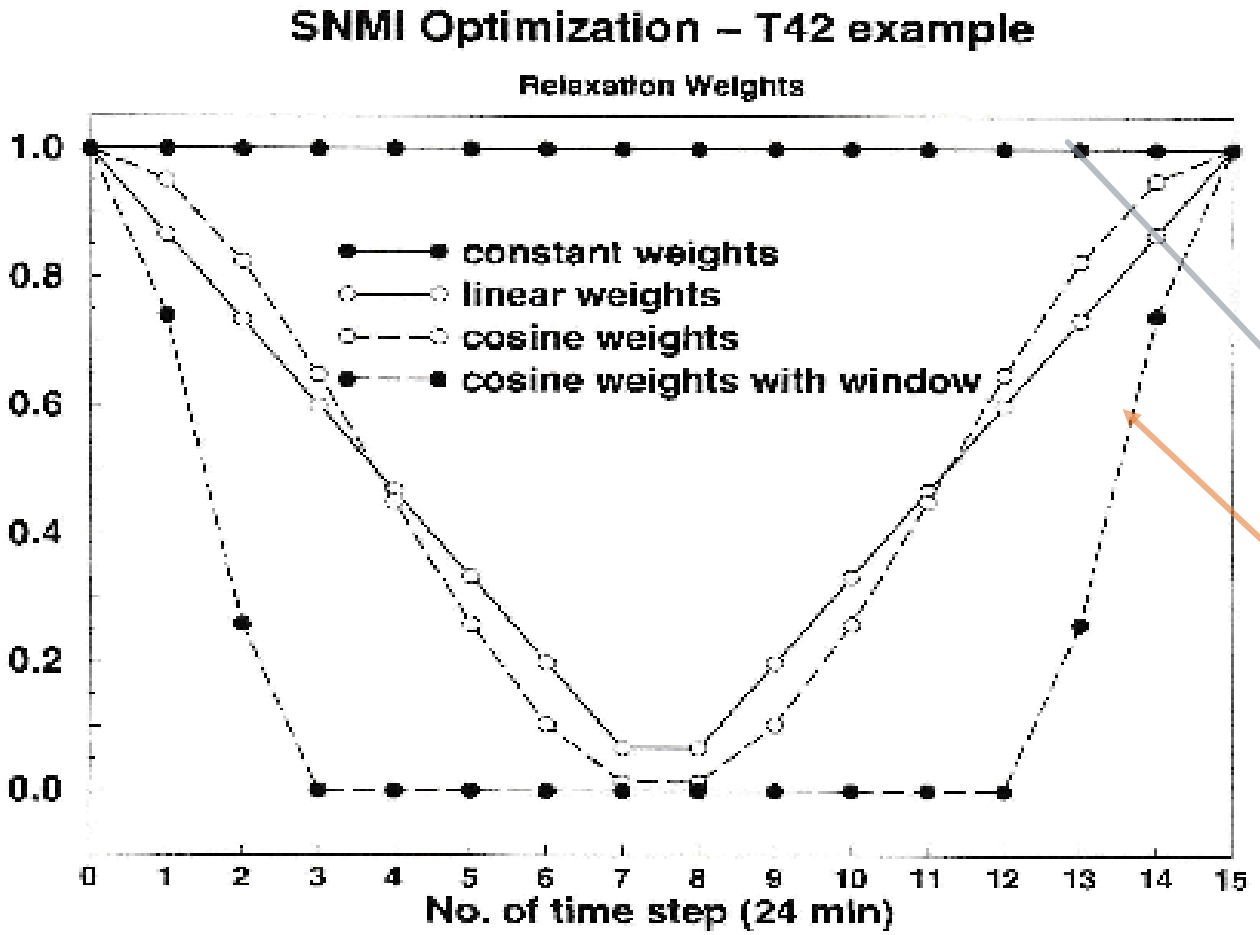

Figure 3
Relaxation weights as a function of time.

SLIDE 6

IF THE Relaxation weight μ(t)<1 only the fraktion μ of the slow normal modes are inserted.

Here μ(t) is a function of time step number between two synoptic times

- **We have tested two SNMI versions:**
  - **Full(SNMI) with constant μ=1**
  - **Opt(SNMI) with μ cosine shaped around synoptic times and a "window" with μ=0 between.**

SLIDE 7:

The traditional *NODGING* technique (Jeuken et al., 1996) is defined as follows:

$$\frac{\partial X_i}{\partial t} = F_i(X_1, X_2, \ldots, X_N) + G_i \times (X_{OBS,i} - X_i)$$

In a three level scheme :

$$X_i^{n+1} = X_i^{n-1} + 2\Delta t F_i^n(X_1^n, X_2^n, \ldots, X_M^n) + 2\Delta t G_i \times (X_{OBS,i}^{n+1} - X_i^{n+1})$$

or

$$X_i^{n+1} = \mu_i \times X_{OBS,i}^{n+1} + (1 - \mu_i) \times X_{m,i}^{n+1} \quad (1)$$

where $\mu_i = \frac{2\Delta t G_i}{1 + 2\Delta t G_i}$ and

$$X_{m,i}^{n+1} = X_i^{n-1} + 2\Delta t F_i^n(X_1^n, X_2^n, \ldots, X_M^n)$$

Table 1: Relaxation coefficients in *DMI nudging*

Prognostic variable,

X_i	μ_i	τ_i
Vorticity	0.118	6.00 hours
Temperatur e	0.032	24.00 hours
log P_s	0.032	24.00 hours
Divergence	0.016	48.00 hours

where $\tau_i = \frac{1}{G_i}$ is the relaxation time

The third NODGING version is the so called *DMI nudging*. It was developed at the Danish Meteorological Institute by Eigil Kass et al. (2000). The intension was to develop a scheme work ing approximately as the SNMI scheme, without having to separate between slow and fast modes. By using a low nudging or relaxation coefficient for temperature, log pressure and especially divergence and a high one for vorticity the relaxation should be mainly towards Rossby modes

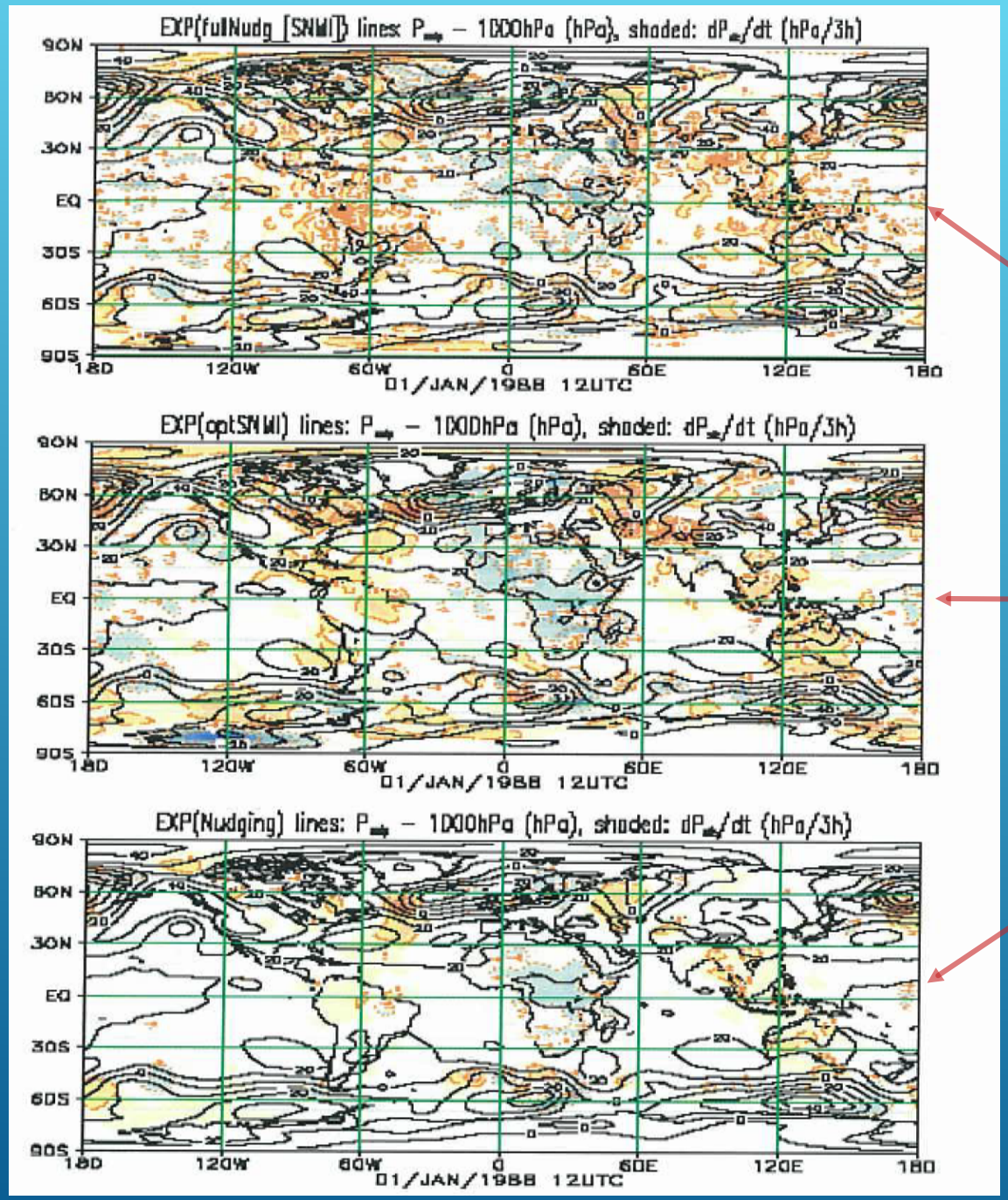

SLIDE 8

COMBINED SURFACE PRESSURE TENDENCIES (SHADED) AND MEAN SEA LEVEL PRESSURE (CURVES).

(A) ***Full(SNMI)*** nudging (μ=1)

(B) ***Opt(SNMI)***

(C***) DMI nudging***

IT MAY BE SEEN THAT OPT(SNMI) (B) HAS THE MOST REALISTIC PRESSURE TENDENCY PATTERN,

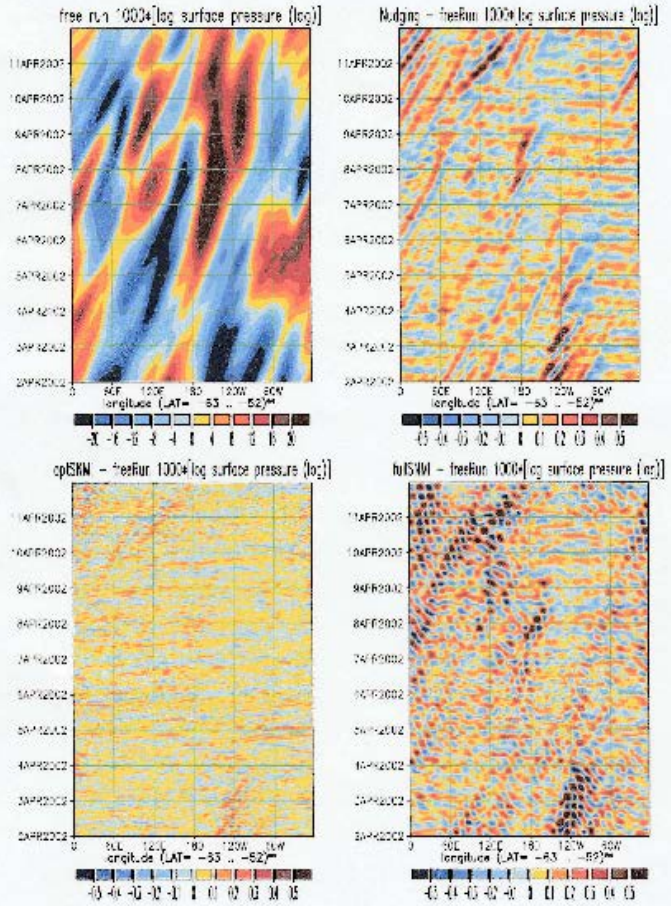

Figure 2a
Hovmoeller diagrams of $1000 \cdot \log p_{surface}$ averaged over the latitude band 63°S to 53°S. Full field in free run (upper left). The rest of the diagrams: deviations from the full free run.

SLIDE 9: THE TIME INTERPOLATION ERROR

HOVMØLLER DIAGRAMS OF $1000 \times log(p)_{surface}$ OVER THE LATITUDE BAND 63 DEG S TO 53 DEG S.

(A) FULL FIELD IN FREE RUN. OUTPUT EACH TIME STEP (24 MIN) (UPPER LEFT)

(B) DMI NUDGING – DEVIATIONS FROM FULL FIELD IN FREE RUN (UPPER RIGHT). LARGE DEVIATIONS SEEN BETWEEN THE INPUT TIMES.

(C) OPT(SNMI) - DEVIATIONS FROM FULL FIELD IN FREE RUN (LOWER LEFT). THE DEVIATIONS BETWEEN THE INPUT TIMES ALMOST ELIMINATED.

(D) FULL(SNMI) - DEVIATIONS FROM FULL FIELD IN FREE RUN (LOWER LEFT) LARGE DEVIATIONS SEEN BETWEEN THE INPUT TIMES.

THIS IS AN "INDENTICAL TWIN" EXPERIMENT . THE ECHAM4 MODEL WAS RUN FOR A LONG PERIOD PRODUCING A FINAL PERIOD OF WELL BALANCED MODEL STATES PLOTTED EACH TIME STEP IN (A).
THE OUTPUT FOR EVERY 6 HOUR FROM THIS PERIOD IS THEN ASSIMILATED INTO THE SAME MODEL USING ONE OF THE ASSIMILATING TECHNIQUES DESCRIBED IN THE PREVIOUS SLIDES. DEVIATIONS BETWEEN THESE ASSIMILATIONS AND THE FREE RUN SHOWN IN (A) ARE SHOWN IN (B)-(D), ALSO PLOTTED EVERY TIME STEP

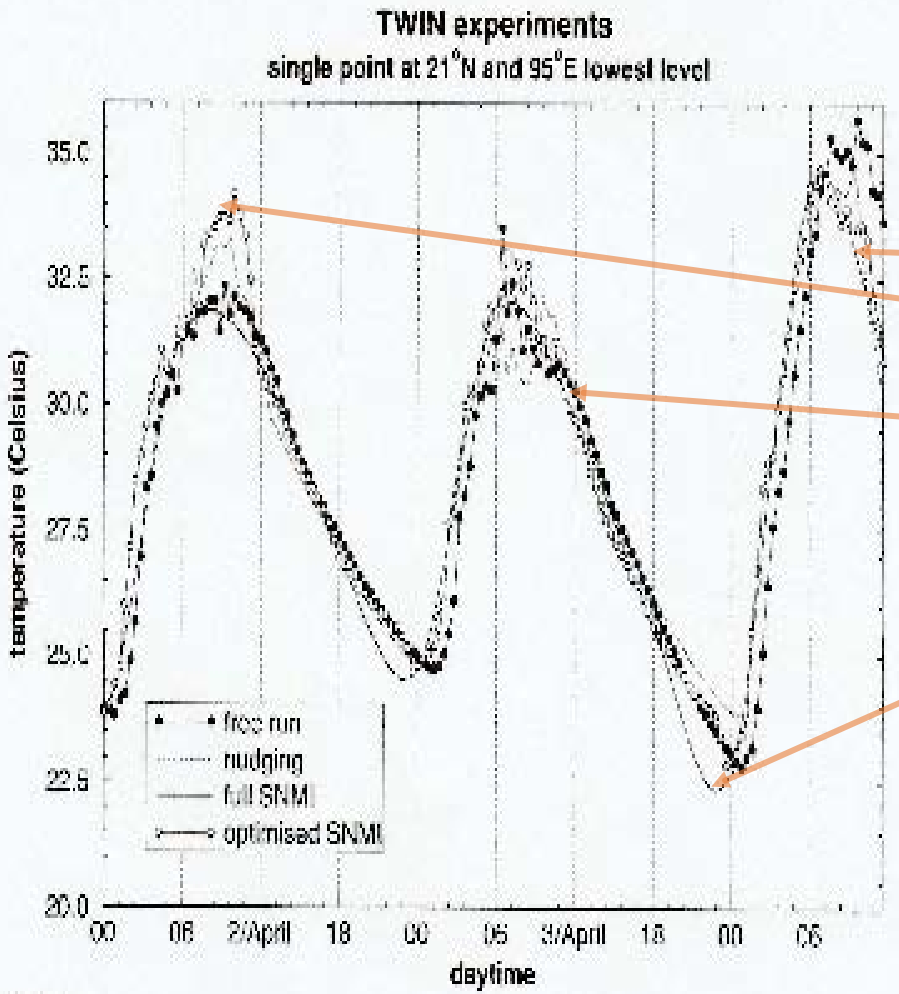

Figure 2b

Temperature at the lowest model level (level 19) at a point over Asia (21°N, 95°E) during a 2.5 days period in April.

SLIDE 10: Improved daily solar cycle

Temperature at the lowest model level (level 19) over Asia (21 deg N, 95 deg E) during a 2.5 day period in April.

Free run

opt(SNMI)

DMI nudging

full(SNMI)

Improvements obtained in the opt(SNMI) compared to the full(SNMI) assimilation is seen in this figure. The full(SNMI) curve follow closely the smooth cubic spline curve (not shown) with a too low and a too early minimum temperature and a too low maximum temperature. The opt(SNMI) curve on the other hand is more realistic especially at the time of the minimum temperature. Also it seems realistic in the sense that, as in the free run now and then excessive temperatures are produced in the opt(SNMI) assimilation, which is important for the release of convection.

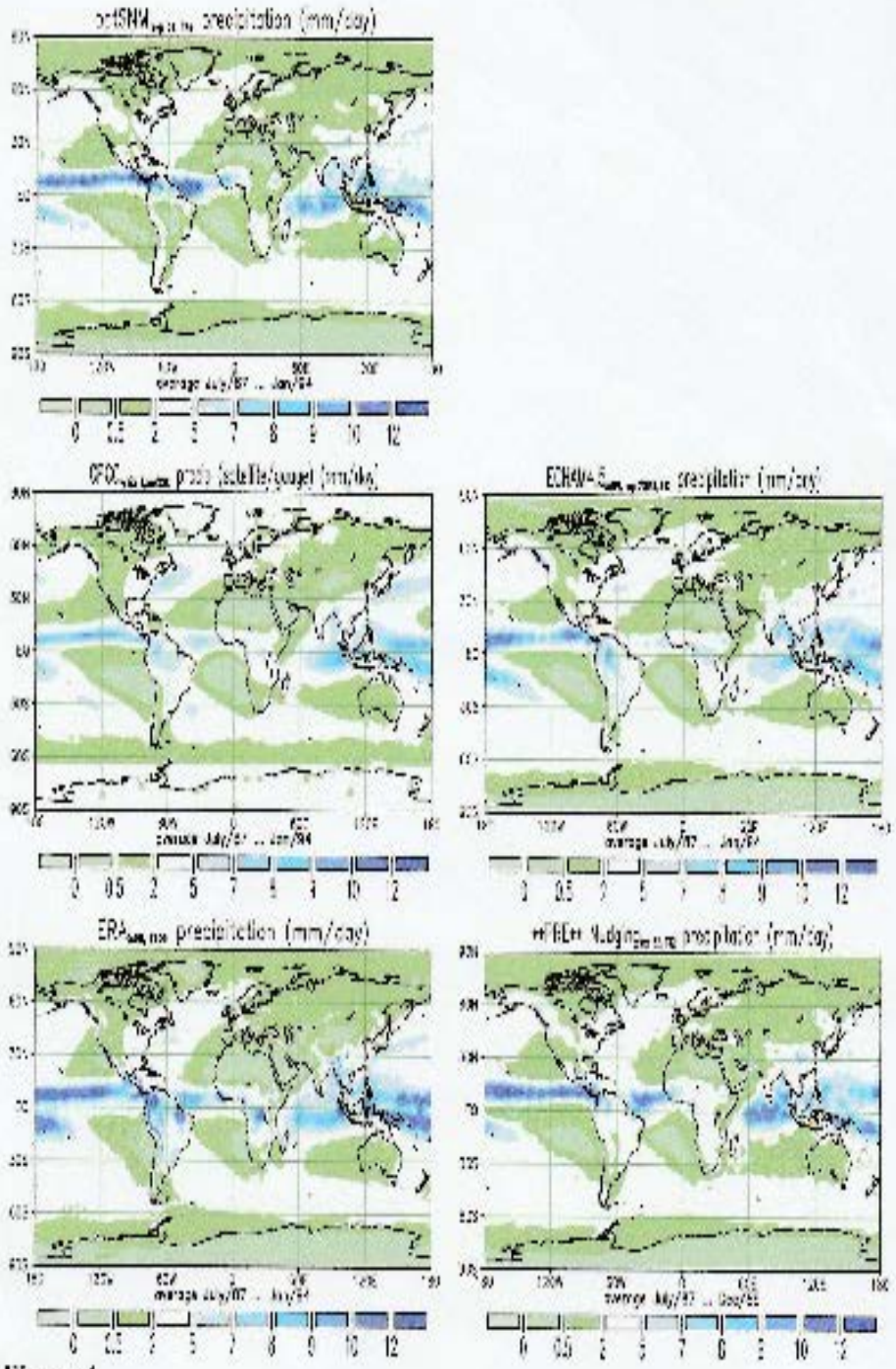

Figure 4

SLIDE 11: Simulation of precipitation

Global precipitation pattern, averaged over the period July 1987 to January 1994.

OPT(SNMI) assimilations (Upper left)

GPCC analyses (middle left)

ECHAM4.5 Amp 2 free simulation (middle right)

ERA 6 hours first guess forecasts (lower left)

DMI nudging assimilations (lower right

Compared to the averaged GPCC analyses generally the opt(SNMI) precipitation is enhanced in the tropics and reduced in middle latitudes, but both deviations are smaller in opt(SNMI) than in full DMI nudging.

A problem is, however, revealed in the opt(SNMI) precipitation map: Over South America only very little precipitation is simulated compared to all the other estimates in the figure. We try to explain this in the next two slides.

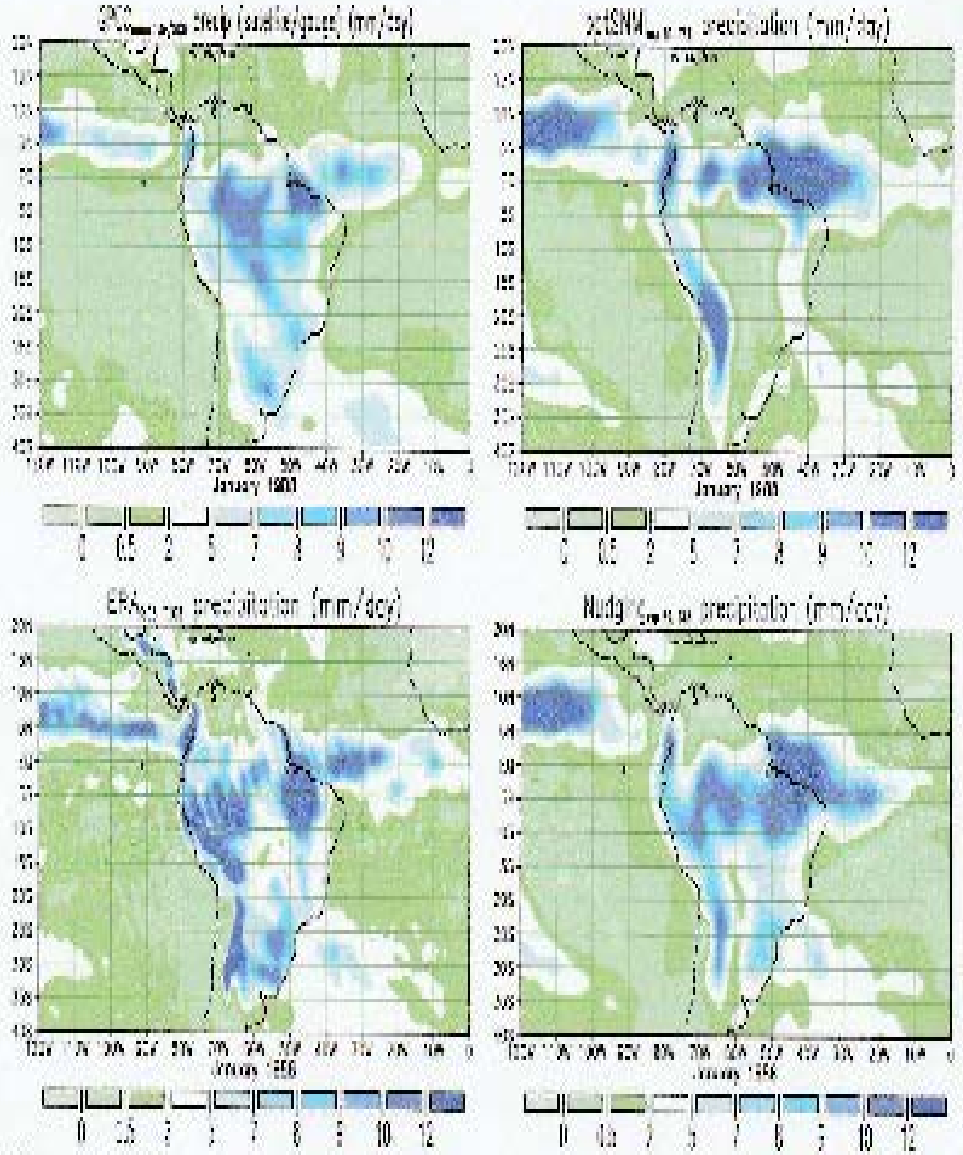

Figure 5

Averaged precipitation over South America during January 1988: GPCC analysis (upper left map), optSNMI assimilation (upper right map), ERA 6 hours first guess forecasts (lower left map), DMI nudging assimilation (lower right map).

SLIDE 12

AVERAGED PRECIPITATION PATTERN OVER SOUTH AMERICA DURING JANUARY 1988.

A) GPCC ANALYSES (UPPER LEFT)

B) OPT(SNMI) ASSIMILATIONS (UPPER RIGHT)

C) ERA 6 HOURS FIRST GUESS FORECASTS (LOWER LEFT)

D) DMI NUDGING ASSIMILATIONS (LOWER RIGHT)

Also for this single month averaged precipitation we get very little precipitation over South America with the opt(SMNI) assimilation (MAP B).

Again this is not the case with DMI assimilation (MAP D). Here the precipitation pattern look similar to the T106 ERA 6 hour first guess forecast precipitation pattern (MAP C), except that it is truncated to T42 resolution.

SLIDE 13

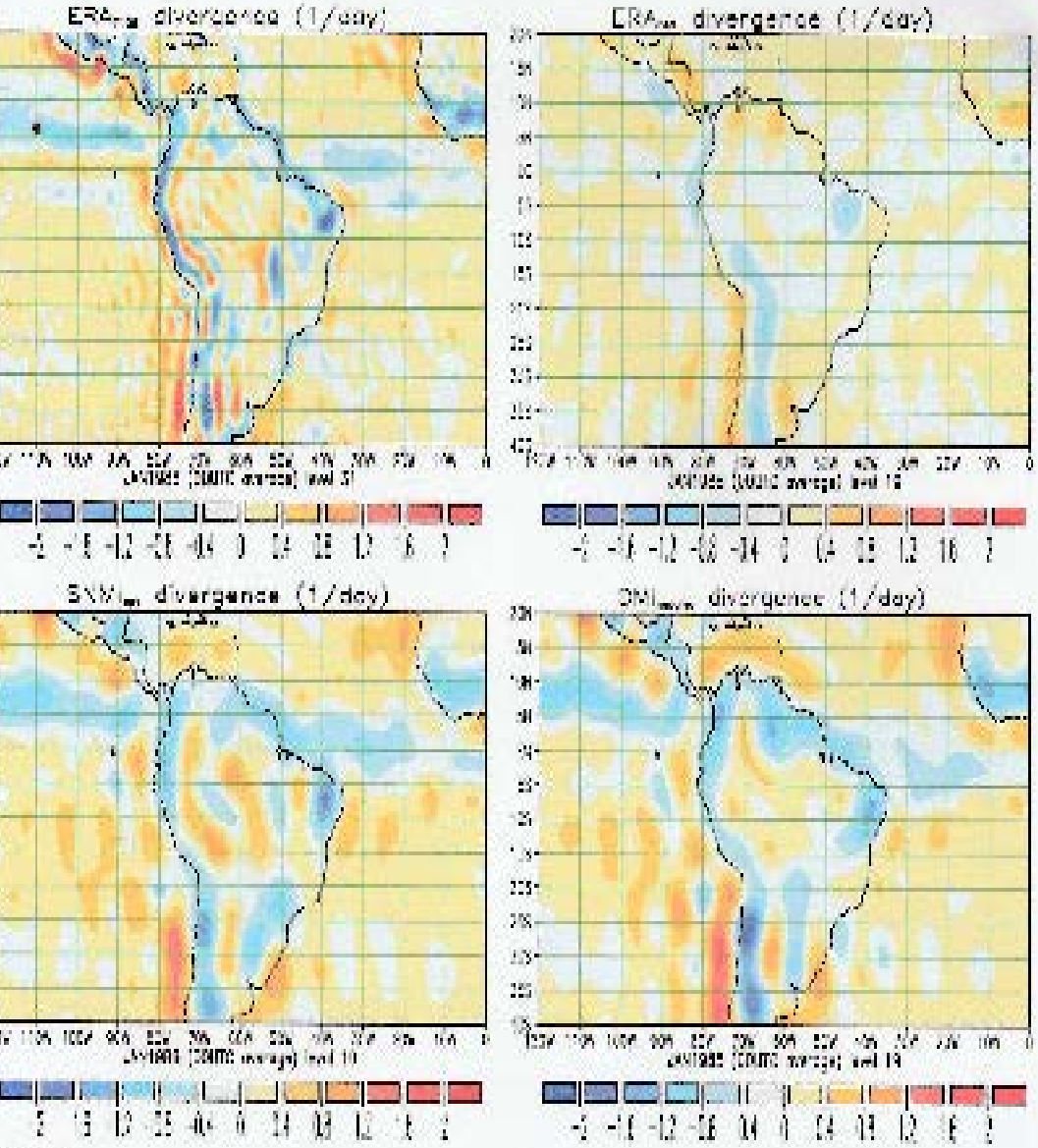

ure 6

LOWEST MODEL LEVEL MONTHLY MEAN DIVERGENCE FIELDS OVER SOUTH AMERICA DURING JANUARY 1988 COMPUTED FROM:

C) ERA T106,L60 6 HOURS FIRST GUESS FORECASTS (LOWER LEFT)

A) ERA T42 (UPPER LEFT)

B) OPT(SNMI) ASSIMILATION (UPPER RIGHT)

D) DMI NUDGING ASSIMILATION (LOWER RIGHT)

A nessesery condition for precipitation is low level convergence. However, when comparing *the time averaged divergence* pattern in the right column of maps (B and D) we see that they are pretty similar. In both cases it is the weak stationary pattern which is developed with the T42 orography. However, the precipitation may be created in stead in connection with individual transient, non-stationary convergence patterns in individual moving synoptic systems. Such consistent small scale divergence patterns must be represented by the fast normal modes, which will only be assimilated by the DMI nudging, Whereas, with opt(SNMI) assimilation these fast modes are not being nudged. Therefore the transient divergence pattern in ERA T42 results only in precipitation in DMI assimilation.

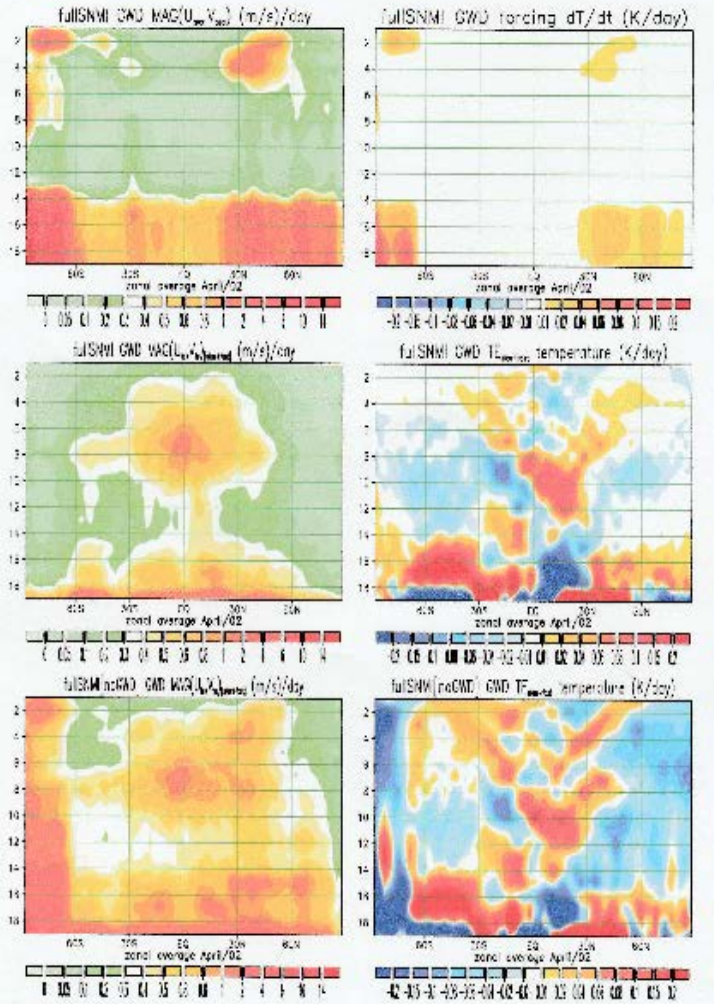

Figure 7

Cross sections of monthly mean zonal averaged tendencies/tendency errors computed from "identical twin" April month input to fullSNMI assimilation. Left column: zonal averaged magnitude of GWD accelerations. Right column: zonal averaged GWD temperature tendency. GWD forcing term (upper row), tendency error with GWD (middle row), and tendency error without GWD (lower row).

MAX ¨TIME INTERPOLATION ERROR":
c) 1.0 m/s/day AND d) 0.10 K/DAY

SLIDE 14

Test of SITE computations with full(SNMI) assimilation

Cross section of mean monthly tendency errors computed from "identical twins" A free ECHAM4 simulated April month is assumed to be "the truth". (comments on SLIDE 14 and SLIDE 15: see SLIDE 16)

A) Zonal averaged magnitude of parametrized GWD acceleration. (upper left)

B) zonal averaged magnitude of parametrized GWD temperature tendency (upper right)

C) zonal averaged magnitude of the estimated acceleration error for an assimilation of the free ECHAM4 simulated April month. (Extreme value : 1 m/s/day) (middle left)

D) zonal averaged estimated temperature tendency error for an assimilation of the free ECHAM4 simulated April month. (Extreme value 0.1 K/day) (middle right

E) zonal averaged magnitude of the estimated acceleration error for an assimilation of an ECHAM4 April month simulation, with a version of ECHAM4 without a GWD parametrization. (lower left)

F) Same as (lower left) but for temperature error. (lower right))

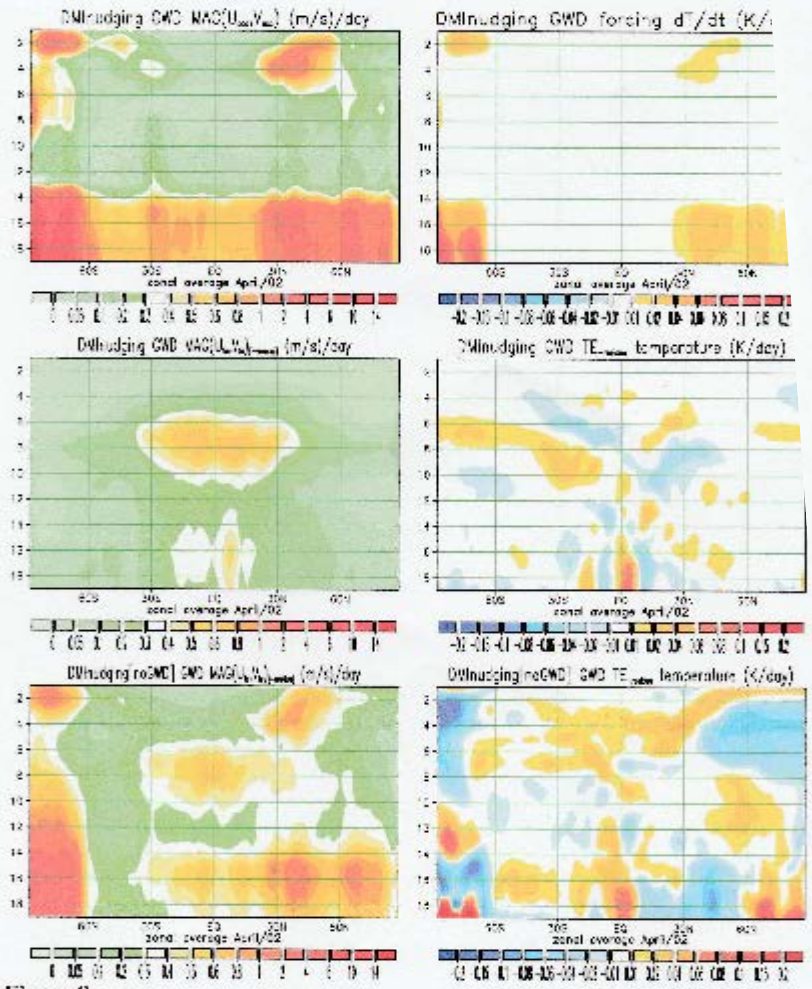

Figure 8
same as Fig.7 but for DMI nudging assimilation.

MAX ¨TIME INTERPOLATION ERROR":
c) 0.6 m/s/day AND d) 0.08 K/DAY

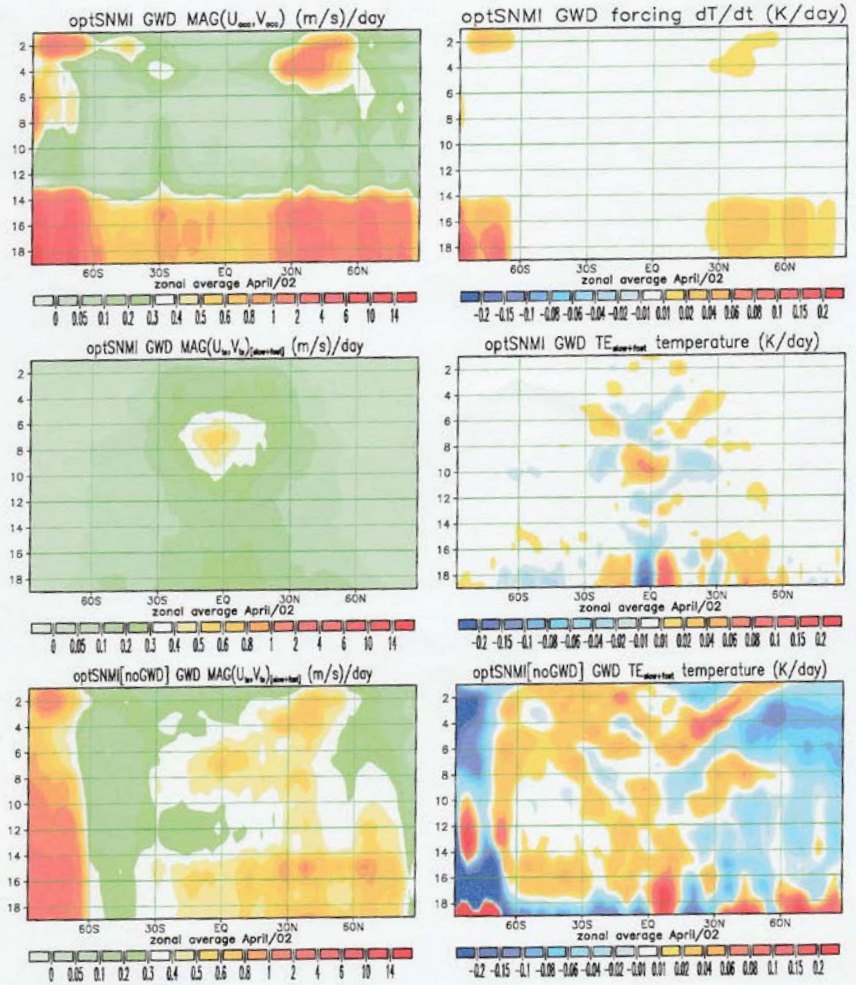

Figure 9
same as Fig.7 but for optimal Slow Normal Mode Insertion.

MAX ¨TIME INTERPOLATION ERROR":
c) 0.5 m/s/day AND d) 0.08 K/DAY

SLIDE 15

Same as FIGURE 14

but for

DMI nudging

and for

Opt(SNMI)

Respectively

In SLIDE 14 and 15 the estimation of SITEs by the SNNI and the DMI nudging techniques was tested and compared in "identical twin" experiments:

A free ECHAM4 simulated April month was taken as the trues. Six hourly output from this simulation was assimilated into the ECHAM4 model and SITEs were computed for each of the assimilation techniques. Ideally these SITEs should be zero but because the non-perfect time interpolation between the available FOUR DAILY SYNOPTIC TIMES they are not zero.

In SLIDE 14 and 15 are shown cross sections of monthly mean zonal averaged tendency errors for the different assimilation methods. In each of the figures are shown in the middle row to the left (C): The zonal averaged magnitude of the estimated acceleration error and in the same row to the right (D:) the zonal averaged temperature tendency error.

For the full(SNMI), the DMI nudging and the obt(SNMI) technique the maximum mean acceleration error is 1.0, 0.6, and 0.5 m/s/day, respectively. And the maximum mean temperature error is 0.10,0.08 and 0.08 K/day, respectively.

The SITEs are compared with the mean value of the Gravity Wave Drag (GWD) which were implemented in ECHAM4 and applied in the April simulation. In the upper row to the left (A) is shown the monthly mean zonal averaged GWD acceleration and to the right (B) the corresponding temperature tendency. Comparing the acceleration errors in (C)/(D) whit those in (A)/(B) we see that the time truncation acceleration errors are only between two and three times smaller than the GWD accelerations and the time truncating heating rates are of the same order of magnitude as the GWD heating rates. *So, the time truncation errors are not insignificant compared to GWD and as seen in the bottom cross sections of the figures it would be difficult to detect a missing GWD parameterization in a model using any of the SITE techniques tested here.*

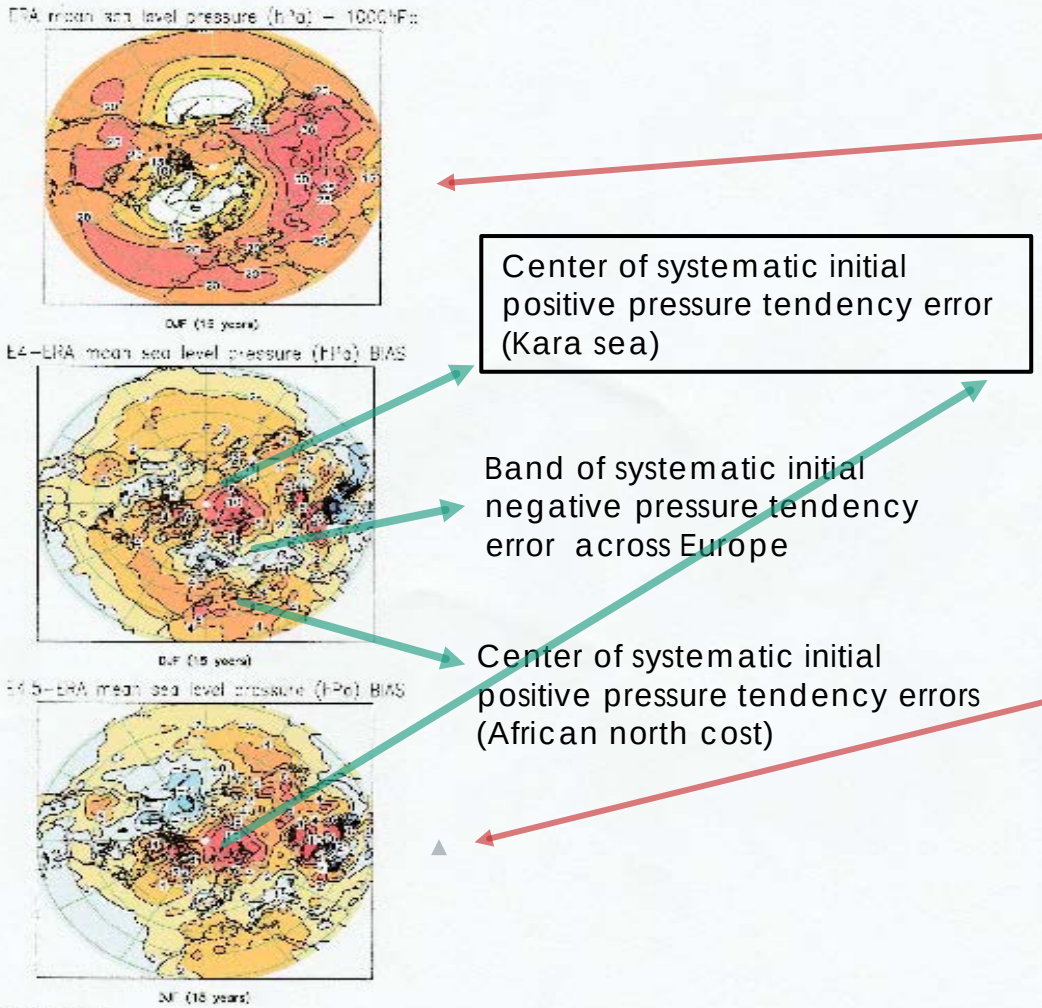

Figure 10
Average winter (DJF) mean sea level pressure (MSLP) for the full 15 years ERA period (upper map) and corresponding systematic MSLP errors (biases) for AMIP2 simulations with the two latest ECHAM model versions, ECHAM4 (middle map), and ECHAM4.5 (lower map)

Center of systematic initial positive pressure tendency error (Kara sea)

Band of systematic initial negative pressure tendency error across Europe

Center of systematic initial positive pressure tendency errors (African north cost)

SLIDE 17

Surface Pressure SITEs

UPPER MAP: AVERAGED WINTER (DJF) MEAN SEA LEVEL PRESSURE (MSLP) FOR THE FULL 15 YEAR PERIOD (UPPER MAP) AND

MIDDEL AND LOWER MAPS: CORRESPONDING SYSTEMATIC INITIAL MSLP TENDENCY ERRORS (SITEs) FOR AMIP 2 SIMULOATIONS WITH THE

ECHAM4 MODEL (MIDDEL MAP)

AND

ECHAM4.5 MODEL (LOWER MAP)

NOTE THE SITEs MARKED IN THE MIDDEL AND THE LOWER MAP (BLUE ERROWS):
Center of positive pressure SITEs over Kara Sea
Band of negative pressure SITEs over Europe
Center of positive pressure SITE over coast of Africa
NOTE THAT:
The band of negative pressure SITEs in ECHAM4 across Europe as well as the center of positive pressure SITEs over the North Coast of Africa has been reduced in the new version, ECHAM4.5.
The center of positive pressure SITEs over the Kara Sea, on the other hand, has increased in the new model version.

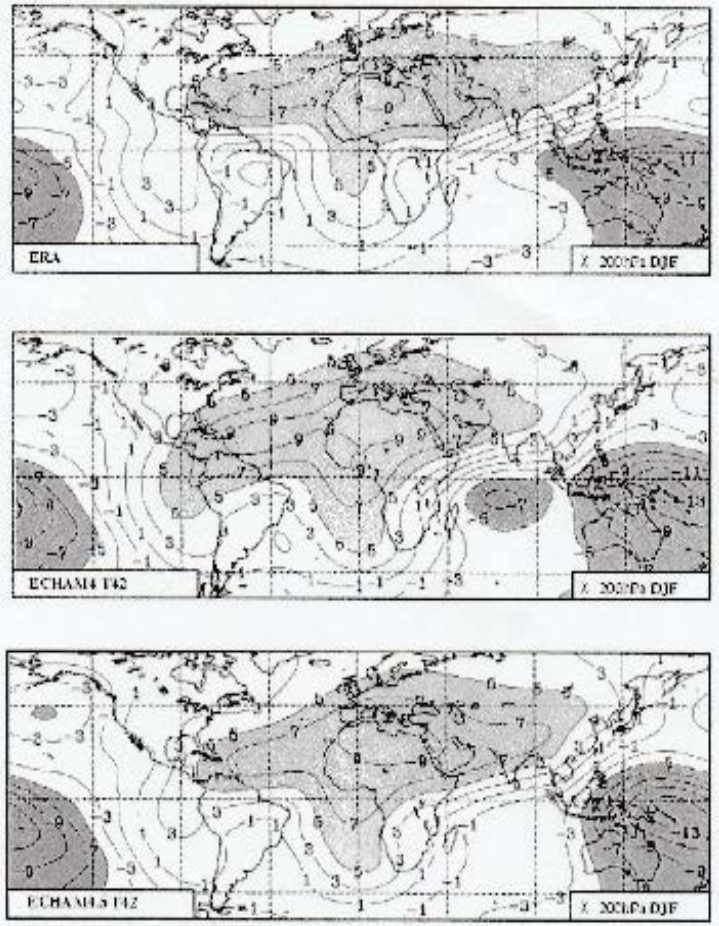

Figure 14
Averaged winter time (DJF) 200 hPa velocity potential for the ERA (upper map), for an ECHAM4 AMIP simulation (middle map) and for an ECHAM4.5 assimilation.

SLIDE 18: REASON FOR THE IMPROVEMENTS NOTED IN SLIDE 17:

AVERAGED WINTER TIME (DJF) 200 HPA VELOCITY POTENTIAL

FOR THE ERA ,

FOR AN ECHAM4 AMIP SIMULATION

FOR AN ECHAM4.5 AMIP SIMULATION

NOTE that: All three maps show an inflow center situated in the upper troposphere above the place over the African north coast where the surface pressure in the model simulations are systematically too high compared to the mean ERA analysis, which we assume are correct. The strength of the inflow is strongest in the ECGAM4 simulation, but is reduced in the ECHAM4.5 simulation. This has lead to a reduced (and more correct) surface pressure in the region in the ECHAM4.5 simulation. Just as we observe. The reduced outflow at low levels will reduce the convergence toward the band of loo low pressure across Europe and thereby weaken the too low pressure band, just as we observe in SLIDE17..

But why is the inflow in 200 hPa reduced in ECHAM4.5 ? The reason will be explained in the next slide.

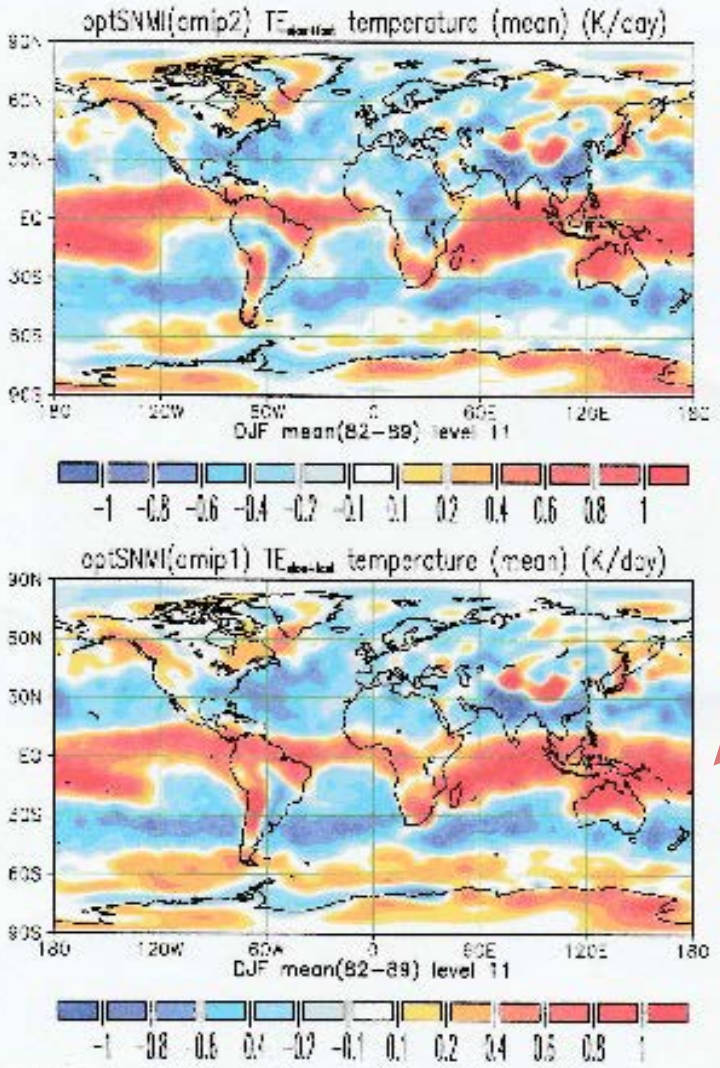

Figure 15

STEs for temperature at level 11 (≈ 500 hPa) based on eight years (1982-1989) of

SLIDE 19: REASON FOR THE IMPROVEMENTS IN SLIDE 17:

SITE'S FOR TEMPERATURE AT LEVEL 11 (~500 HPA) BASED ON 8 YEARS (1982-1989) OF ERA ASSIMILATION USING THE OPT(SNMI) TECHNIQUE IN

AN ECHAM4.5 ASSIMILATION (UPPER MAP)

AND

AN ECHAM4 SIMULATION (LOWER MAP).

Note the difference over Central Africa:

Instead of an erroneous systematic heating in ECHAM4 does the upper map show an erroneous systematic cooling in ECHAM4.5. Thus, instead of inducing rising motions in the mean, which will create diverging horizontal flow below the tropopause, which will contribute to the inflow over the north coast of Africa there will in the mean be subsidence over Central Africa, fed by a converging flow below the tropopause, which will weaken the inflow over the north coast of Africa and thereby weaken the too high surface pressure.

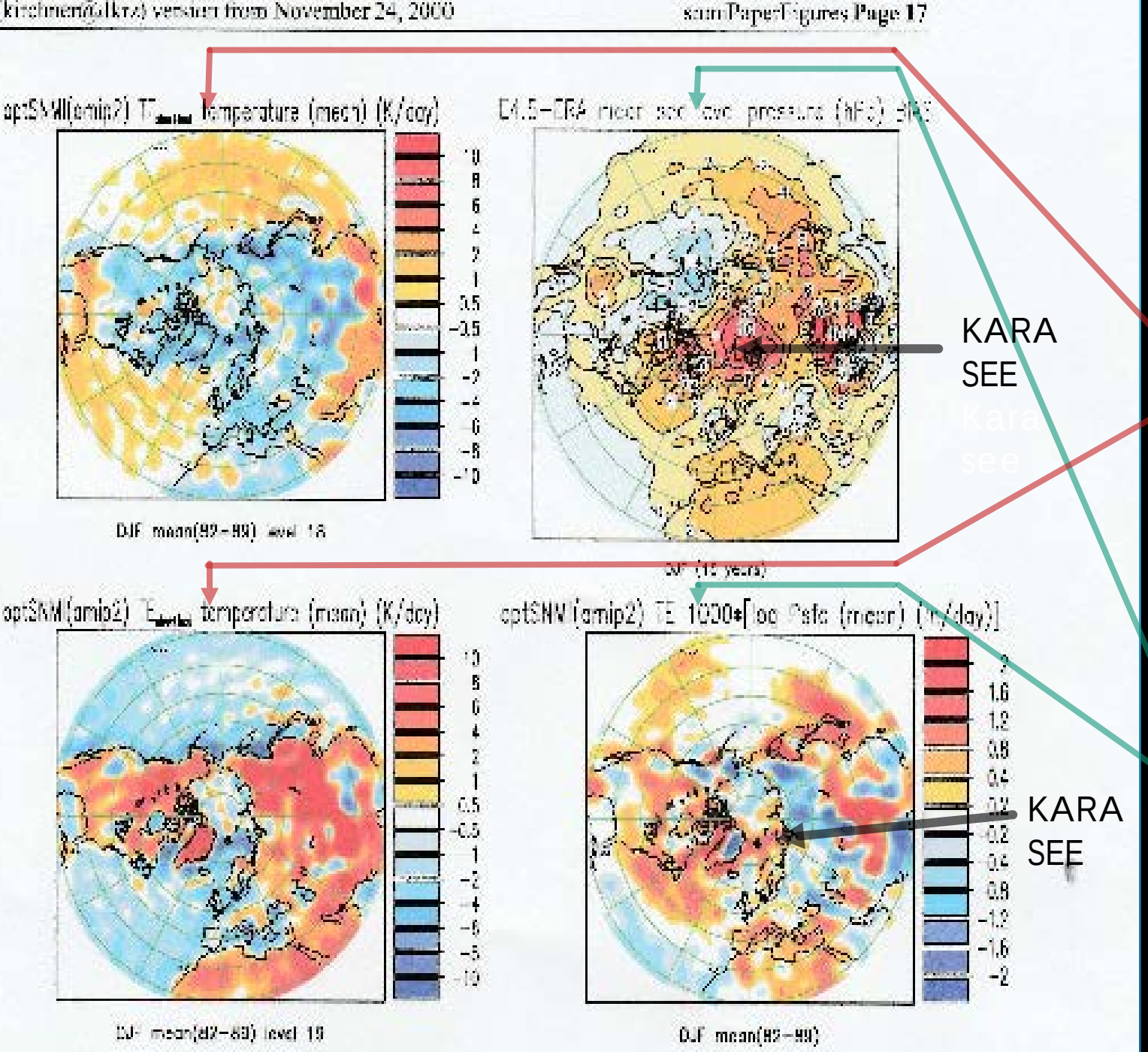

SLIDE 20: THE REASON FOR THE SYSTEMATICALLY TOO HIGH PRESSURE OVER KARA SEA

WINTER SEASON (DJF) TEMPERATURE SITE'S BASED ON EIGHT YEAR (1982-1989) OF AN OPT(SNMI) ECHAM4.5 ASSIMILATION

A) FOR LEVEL 18 (UPPER LEFT MAP)
AND
C) FOR LEVEL 19 (LOWER LEFT MAP).

AT THE LOWEST LEVEL (LEVEL 19) THE MAXIMUM COOLING ERROR IS OVER THE BARENTS SEA AND OVER THE GREENLAND SEA.

AS SEEN IN THE MAP ABOVE THE MAXIMUM COOLING IS SPREADING OUT TO NIGHTBOURING LONGITUDES IN LEVEL 18.

(B) MSLP BIAS OF A 15 YEARS ECHAM4.5 AMIP2 SIMULATION (E4.5 – ERA) (UPPER RIGHT MAP)

D) CORRESPONDING SURFACE PRESSURE SITE'S (LOWER RIGHT MAP).

The maximum cooling errors seen in map C and A is obviously causing the maximum surface pressure SITE in map D which is causing the sur face pressure bias in map B

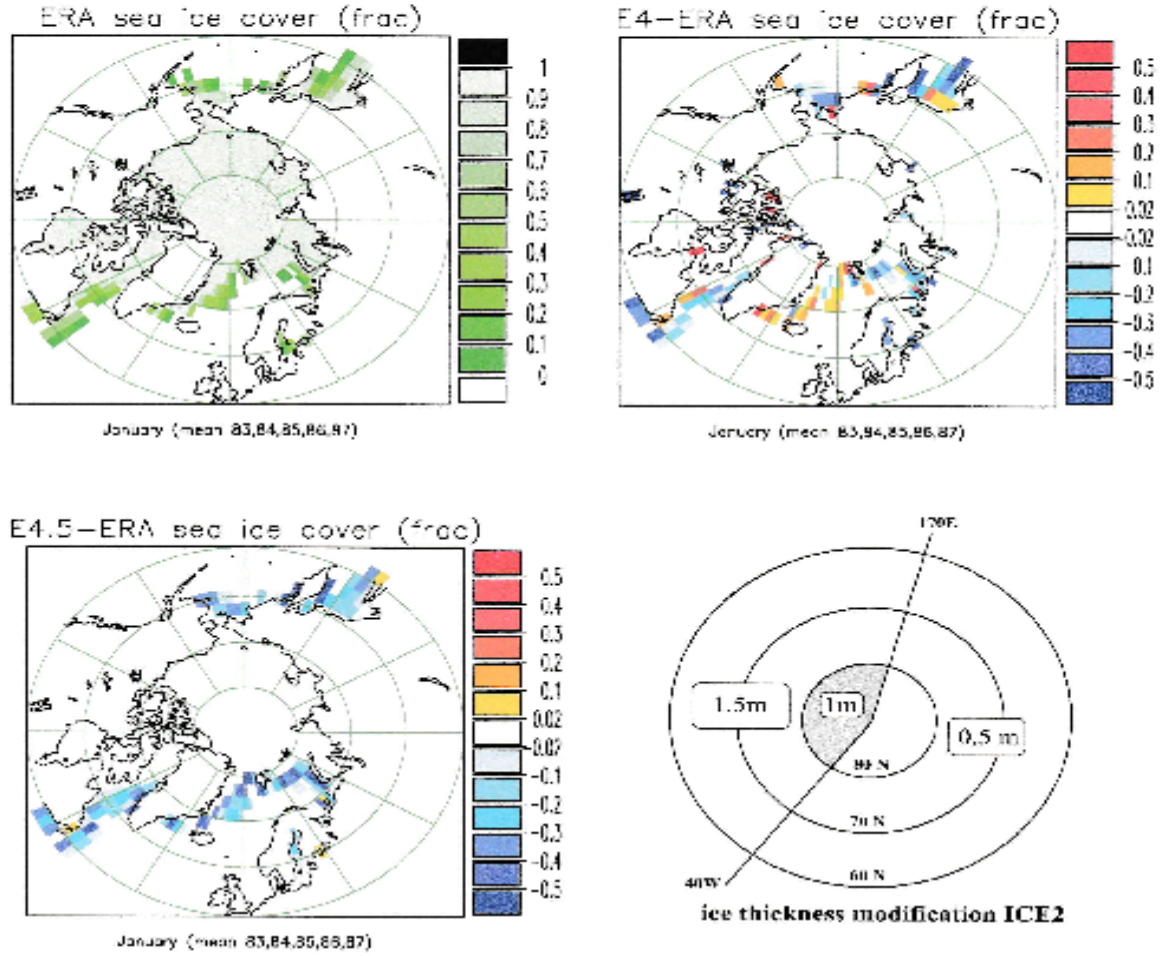

Figure 17
5 year mean January ERA sea ice coverage (upper left map), difference between the AMIP2 sea ice coverage and the ERA sea ice coverage (lower left map), difference between the AMIP1 sea ice coverage and the ERA sea ice coverage (upper right map), and the sea ice thickness in the ICE2 simulation (lower right map)

SLIDE 21
IN THE ERA DAILY SST AND SEA ICE COVERAGE ANALYSES WERE UTILIZED.

A) 5 YEAR (1983-1988) MEAN JANUARY ERA SEA ICE COVERAGE (UPPER LEFT MAP).

IN THE STANDARD AMIP2 ECHAM4.5 SIMULATIONS MONTHLY SST AND SEA ICE COVERAGE WERE USED AND A CONSTANT SEA ICE THICKNESS WERE SET EQUAL TO 1.5 METERS.

C) DIFFERENCE BETWEEN THE FIVE YEAR MEAN JANUARY AMIP2 SEA ICE COVERAGE AND THE FIVE YEAR MEAN JANUARY ERA SEA ICE COVERAGE (LOWER LEFT MAP)

B) DIFFERENCE BETWEEN THE FIVE YEAR MEAN JANUARY ECHAM4 AMIP1 SEA ICE COVERAGE AND THE FIVE YEAR MEAN JANUARY ERA SEA ICE COVERAGE (UPPER RIGHT MAP).

OBVIOUSLY THE SEA ICE COVERAGE HAS BEEN REDUCED FROM ECHAM 4 TO ECHAM 4.5

D) THE SEA ICE THICKNESS IN THE ICE2 SIMULATION (LOWER RIGHT MAP).

TWO 1982-1988 TEST ECHAM4.5 INTEGRATIONS WERE MADE:

ICE1 WITH ERA DAILY SST AND SEA ICE COVERAGE AND A CONSTANT SEA ICE THICKNESS EQUAL TO 1.5 METERS.

AND
ICE2 WITH THE SAME SST AND SEA ICE COVERAGE AS ICE1 BUT WITH THE SEA ICE THICKNESS SHOWN IN FIGURE D.

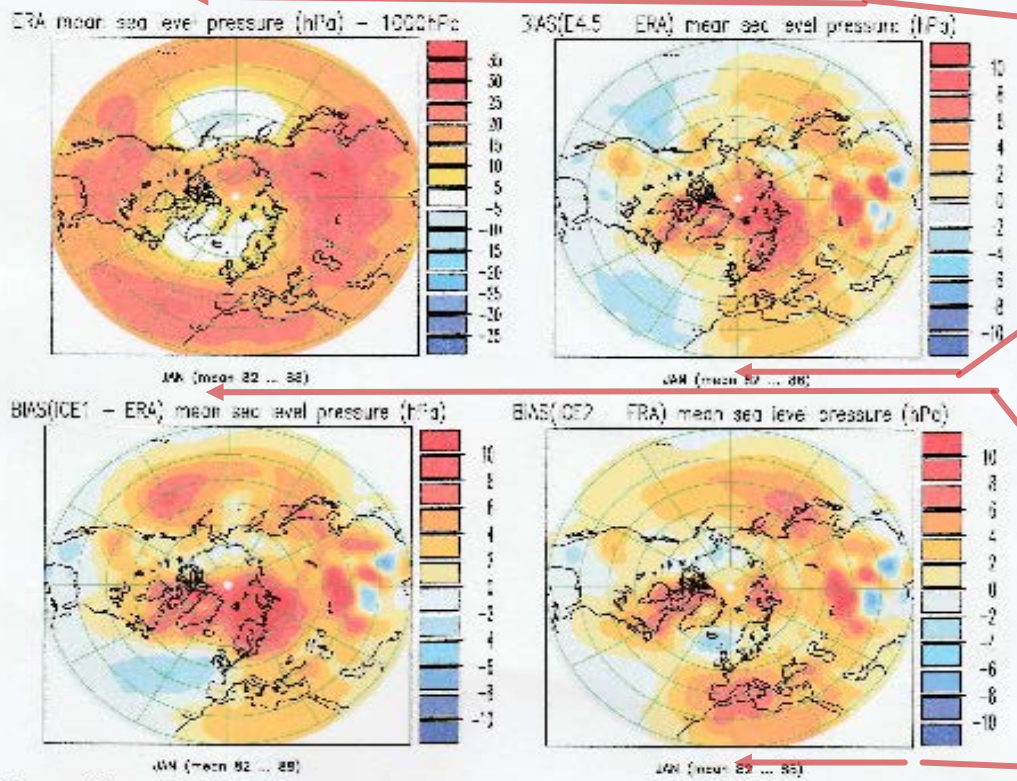

Figure 18
7 year mean ERA January MSLP distribution over the Arctic (upper right map), and corresponding systematic MSLP error patterns for the AMIP simulation (upper right map), for the ICE1 simulation (lower left map), and for the ICE2 simulation (lower right map).

SLIDE 22

A) ERA: 7 YEAR MEAN JANUARY MSLP DISTRIBUTION OVER THE ARCTIC
(UPPER LEFT)

B) CORRESPONDING MSLP SITE (SYSTEMATIC INITIAL TENDENCY ERROR) PATTERN FOR THE ECHAM4.5 AMIP SIMULATION (UPPER RIGHT)

TO TEST IF THE TOO HIGH PRESSURE OVER THE KARA SEA IS DUE TO TOO LARGE SEA ICE COVERAGE AND TOO THICK SEA ICE COURSING TOO LITTLE HEATING FROM THE SEA THE FOLLOWING TWO TEST RUNS WERE MADE:

C) THE ICE1 SIMULATION WITH REDUCED SEA ICE COVER (LOWER LEFT)

D) THE ICE II SIMULATION WITH BOTH REDUCED SEA ICE COVERIDGE AND REDUCED SEA ICE THICKNESS
(LOWER RIGHT)

Results of optSNMI MSLP SITE estimats
The *ICE1 simulation:* relatively small changes. The Kara Sea maximum is slightly intensified, the band of lower pressure across Europe is slightly more pronounced. And the maximum over the African coast is unchanged.
***The ICEII simulation:* here the expected change over the Kara Sea maximum has occurred. At the same time, however, unexpected intensification of the band of too low pressure across Europe and the maximum over the African coast.**

Conclusions (Part 1):

Different nudging techniques were tested to assimilate higher resolution T106,L31 reanalysis data, REA-15, given at 4 synoptic times a day, 06, 12, 18, 24 UTC, into lower resolution T42, L 19 semi implicit climate models, ECHAM4 and ECHAM4.5, with a time step of 24 minutes.
Each reanalysis were at first truncated to the T42 resolution and interpolated to the 19 sigma levels of the climate models. Using cubic splines the data were also interpolated to the 24 minutes time step of the climate models.

With DMI nudging a nudging were made with time independent nudging coefficients, which were constant for each variable but vary from variable to variable in the same way as in external Rossby modes.

With SLOW NORMAL MODE INSERTION (SNMI) only so-called *slow normal modes* are nudged toward the corresponding ERA modes. Here the SLOW NORMAL MODES are defined as the modes with periods larger than 24 hours.

With full(SNMI) all SLOW NORMAL MODE coefficients of the truncated and vertical as well as time cubic interpolated ERA data are inserted every time step for the corresponding SLOW NORMAL MODE coefficients of the climate model. The FAST NORMAL MODES are not nudged, they are predicted as in a free climate run.

CONCLUSIONS (PART 1) CONTINUESD AT NEXT SLIDE:

Conclusion (Part1) continued:

With the opt(SNMI) assimilation all SLOW NORMAL MODE coefficients of the truncated and interpolated ERA data are inserted for the corresponding SLOW NORMAL MODE coefficients of the climate model, but only at and around the 4 REA synoptic analysis times. The nudging coefficient is decreasing to zero between the analysis times. (as illustrated at SLIDE 7). The FAST NORMAL MODES are not nudged, they are predicted as in a free climate integration

A series of experiments have shown the superiors performance of the obt(SNMI) assimilation technique compared with the other too techniques:

- **The twin experiments presented in SLIDE 10 showed that *a realistic daily solar cycle for the surface temperature* was obtained with obt(SNMI).**
- **The *cubic spline time interpolation error* were monitored at first in SLIDE 9. It was shown that with obt(SNMI) the error between the synoptic input times were almost eliminated and**
- **in SLIDE 14 and 15 we showed cross sections of monthly mean zonal averaged wind and temperature tendency errors caused by the time interpolation errors for the different assimilation methods. The smallest tendency errors were found with obt(SNMI)**
- **The induced acceleration error were between two and four times smaller than the parameterized gravity wave drag (GWD) acceleration and the interpolation heating rate error were seen to be of the same order of magnitude as the GWD heating rates. Thus, it would be difficult to detect a missing GWD parameterization from a SITE analysis. However the GWD parameterization is weak compared to other parameterizations.**

In SLIDE 8 it was shown that the obt(SNMI) assimilation technique gave the most realistic surface pressure tendency fields compared to similar fields obtained with the two other assimilating techniques, because apparently long period gravity modes (external modes with periods longer than 24 hours) with strong vertically integrated divergence fields in the ERA data were assimilated better with obt(SNMI).

Some kinds of precipitation may on the other hand develop from low level convergence fields in particular. Such fields will be represented by fast gravity modes which are not nudged in obt(SNMI) assimilations as shown in obt(SNMI) assimilations of at first an 8 years ERA-15 analyses and more clearly of a January 1988 analysis considered in SLIDS 11-13. The assimilations also show that they do not develop in the freely model predicted fast gravity modes with the obt(SNMI) assimilation, As a result In the case considered no precipitation develops over Brazil. with the obt(SNMI) assimilation.

***This is a severe problem for the obt(SNMI) assimilation*.**

A similar DMI nudging assimilation of the same ERA-15 analysis considered in SLIDS 11-13 gave precipitation similar to the ERA T42 analysis.

Finally in SLIDE 17-23 it was shown how mayor surface pressure SITEs can be detected in a climate model

Finally in SLIDE 17-23 it was shown how mayor surface pressure SITEs (causing a center of too high pressure over the Kara Sea, a band of too low pressure across Europe and a center of too high pressure over the North African Cost) could be detected in the ECHAM4. It was shown how the reduction of the release of latent heat in the ITTC over AFRICA in the new version, the ECHAM4.5, had resulted in a weakening of the center of too high pressure over the North African Cost as well as reduced the too low pressure in the band across Europe. Finally, experiments with the observed reduced extend of sea ice over the Arctic Ocean and at the same time a reduction of the thickness of the sea ice were reported on. The result of this experiment was as expected that the center of too high pressure over the Kara Sea were almost eliminated. At the same time, however, unexpected intensification of the band of too low pressure across Europe and the center of too high pressure over the African Coast took Place.

Final Part 1 conclusion:

The conclusion from PART 1 is that in general the SITE detection by the obt(SNMI) technique works satisfactory and generally better than the DMI nudging technique. The purpose of the obt(SNMI) technique is to assimilate higher resolution ERA data (here with resolution T106,L31) given at four synoptic times a day, into lower resolution climate models (here with resolution T42, L19) with a time step of 24 minutes. This involves truncation and interpolation which tend to introduce noise that typically is represented by fast gravity modes. To avoid such noise we are nudging only Slow Normal Modes with periods longer than 24 hours. Thus we can use obt(SNMI) except when we wont to detect low level divergence fields which are represented by fast modes. In that case the DMI technique should be preferred. However, small scale divergence fields in the T106,L31 resolution will not be realistically represented in T42,L19 resolution.